Journal of Pharmaceutical and Biomedical Analysis 148 (2018) 182–188

Contents lists available at ScienceDirect

Journal of Pharmaceutical and Biomedical Analysis

journal homepage: www.elsevier.com/locate/jpba

Short Communication

Thermal stability study of crystalline and novel spray-dried amorphous nilotinib hydrochloride

Maikel Herbrink[a,*], Herman Vromans[b], Jan Schellens[a,c], Jos Beijnen[a,c], Bastiaan Nuijen[a]

[a] Department of Pharmacy and Pharmacology, Antoni van Leeuwenhoek hospital – The Netherlands Cancer Institute (AvL-NKI), Plesmanlaan 121, 1066 CX, Amsterdam, The Netherlands
[b] Department of Pharmaceutical Sciences, Utrecht University, Universiteitsweg 99, 3584 CG, Utrecht, The Netherlands
[c] Division of Pharmacoepidemiology and Clinical Pharmacology, Science Faculty, Utrecht Institute for Pharmaceutical Sciences, Utrecht University, Universiteitsweg 99, 3584 CG, Utrecht, The Netherlands

ARTICLE INFO

Article history:
Received 6 June 2017
Received in revised form
18 September 2017
Accepted 1 October 2017
Available online 12 October 2017

Keywords:
Amorphous
Spray drying
Thermal analysis
Stability
Thermodynamics

ABSTRACT

The thermal characteristics and the thermal degradation of crystalline and amorphous nilotinib hydrochloride (NH) were studied. The spray drying technique was successfully utilized for the amorphization of NH and was evaluated by spectroscopic techniques and differential scanning calorimetry (DSC). The ethanolic spray drying process yielded amorphous NH with a glass transition temperature (T_g) of 147 °C.

Thermal characterization of the amorphous phase was performed by heat capacity measurements using modulated DSC (mDSC). Thermal degradation was studied by thermogravimetric analysis (TGA).

The derived thermodynamic properties of the amorphous NH indicate fragile behaviour and a low crystallization tendency.

NH was found to be molecularly stable up to 193 °C. After which, the thermal degradation displayed two phases. The values of the thermal degradation parameters were estimated using the Ozawa-Flynn-Wall and Friedman non-isothermal, model-free, isoconversional methods The results indicate the two phases to be single-step reactions.

The examination of the physical stability of amorphous NH during storage and at elevated temperatures showed stability at 180 °C for at least 5 h and at 20–25 °C/60% RH for at least 6 months. During these periods, no crystallization was observed.

This study is the first to report the thermal characteristics of NH. Additionally, it is also the first to describe the full thermal analysis of a spray-dried amorphous drug. The thermal data may be used in the projection of future production processes and storage conditions of amorphous NH.

1. Introduction

The tyrosine kinase inhibitor nilotinib hydrochloride (NH) (see Supplementary Fig. S1 in the online version at DOI: 10.1016/j.jpba.2017.10.001) is registered for the treatment of newly diagnosed adults with Philadelphia chromosome positive myeloid leukemia (Ph+ CML) in the chronic phase. It is also indicated for the treatment of chronic and accelerated phase Ph+ CML in adult patients that are resistant or intolerant to prior therapy that included imatinib [1].

The oral dosage form of NH (Tasigna®) contains the crystalline polymorph B and is associated with poor solubility and permeability that hinders its bioavailability [2]. Solubility and bioavailability improvement of drugs may be achieved by formulating the amorphous form. Although the amorphous form is often less stable than the crystalline polymorphs, it tends to exhibit improved dissolution characteristics [3].

A nanoparticle formulation containing amorphous NH have been shown to markedly increase the solubility of the drug [4]. Furthermore, another study with this formulation demonstrated an increase in the human bioavailability and shows the advantages of utilizing the amorphous form [5].

Amorphous drug can be manufactured from crystalline material by usage of a large variety of techniques. The spray drying tech-

Abbreviations: NH, nilotinib hydrochloride; OFW, ozawa-flynn-wall; F, Friedman.

* Corresponding author.
E-mail address: m.herbrink@nki.nl (M. Herbrink).

https://doi.org/10.1016/j.jpba.2017.10.001
0731-7085/

nique was chosen for this study because it enables relatively short production times, large- and small-scale productions and due to its setting flexibility [6]. Additionally, spray drying has successfully been applied in the development and production of various formulations that contain amorphous drugs [7]. The use of the spray-drying technique for the production of amorphous NH has not been reported previously in literature.

The application of thermal analysis methods is important in the pharmaceutical industry, especially in cases where amorphous forms are involved [8]. The methods can be used in studies of polymorph stability, crystallization, stability, compatibility and kinetic parameters. The thermal properties may determine the choice of production methods, storage conditions, bioavailability and by extension, therapeutic efficiency [9]. Additionally, formulation development that follows Quality by Design (QbD) principles should include a full assessment of drug characteristics [10]. This approach will allow for critical drug properties to be identified timely.

For these reasons, it is of importance to study the thermal characteristics and thermal stability of the amorphous form and the crystalline polymorph from which it is produced. No information is available in literature about the thermal behavior of either crystalline or amorphous NH. Furthermore, a full thermal and thermodynamic analysis of a spray-dried amorphous drug has also not been reported before. This study is the first to perform these analyses and establish these characteristics.

The spray-drying process was evaluated by ^{1}H- and ^{13}C-Nuclear Magnetic Resonance spectroscopy (NMR), Fourier transform infrared spectroscopy (FTIR), powder X-ray diffraction (XRD) and differential scanning calorimetry (DSC). The thermal characteristics of the amorphous state of NH were assessed using modulated temperature DSC (MTDSC). The thermal stability and degradation of NH were studied with thermogravimetric analysis and were evaluated by the non-isothermal, isoconversional Ozawa-Flynn-Wall (OFW) and Friedman (F) methods as is recommended by the International Confederation for Thermal Analysis and Calorimetry [11].

The results from this study may be used in the quality control of both crystalline and amorphous and may play a role in the design of production processes and the choice of storage conditions.

2. Materials and methods

2.1. Materials

NH monohydrate was purchased from Avachem Scientific (San Antonio, TX, USA) and was supplied with a certificate of analysis. All analyses were compared to a reference standard to exclude any batch-to-batch differences. The reference standard of NH (monohydrate) was acquired from AlsaChim (Illkirch, France). All other chemicals were of analytical grade. Residual solvents (<0.5%) were detected by gas chromatography. Moisture content was determined by Karl Fisher titration.

2.2. Amorphous phase preparation

The amorphous phase of the compound was prepared by the spray drying technique using a Büchi MiniSpray Dryer B-290, Inert Loop B-295, High performance cyclone, 1.5 mm nozzle cap and 0.7 mm nozzle tip (Büchi). Spray dry system settings were: Spray feed 20%; N_2 atomization flow 40 mm; aspirator flow 100%; inlet temperature 120 °C; outlet temperature 75 °C; inert loop temperature −20 °C. NH monohydrate (10 g/L) was dissolved in 100% ethanol and the solution was stirred using a magnetic stirrer at 20–25 °C.

2.3. ^{1}H-, ^{13}C-Nuclear magnetic resonance spectroscopy (NMR)

NMR spectra were recorded with an Avance Ultrashield instrument (Bruker Corporation, Billerica, MA, USA). The ^{1}H NMR and ^{13}C NMR spectra were recorded at 300 MHz and 75 MHZ, respectively. The samples were dissolved in DMSO (highest peak in multiplet at 2.50 ppm). In the ^{13}C-spectrum, the center peak of the DMSO signal was at 38.5 ppm.

2.4. Fourier transform infrared spectroscopy (FTIR)

FT-IR spectra were recorded from 650 to 4000 cm^{-1} with a resolution of 2 cm^{-1} with a FT-IR 8400S Spectrophotometer equipped with a golden gate® (Shimadzu, 's-Hertogenbosch, the Netherlands). A total of 64 scans were averaged into one spectrum. Data analysis was performed with IR Solution software V1.4 (Shimadzu).

2.5. Powder X-ray diffraction (XRD)

X-ray diffraction of powder samples was performed with an X'pert pro diffractometer equipped with an X-celerator (PANanalytical, Almelo, The Netherlands). Samples were placed in a 0.5 mm deep metal sample holder. Samples were scanned at a current of 30 mA and a tension of 40 kV. The scanning grange was 10–60° 2-θ, with a step size of 0.020° 2-θ and a scanning speed of 0.002° 2-θ per second. The spectra were processed using HighScore software v4.5.

2.6. (modulated) differential scanning calorimetry ((m)DSC)

mDSC and DSC measurements were performed with a Discovery DSC (TA Instruments) equipped with a refrigerating device and suitable for direct heat capacity measurements. Temperature scale and heat flow were calibrated with indium reference disks. Drug samples of approximately 3–5 mg were weighed in Tzero aluminium pans (TA Instruments), compacted, sealed and placed in the autosampler. Each sample was equilibrated at 20 °C, after which the samples were heated with a speed of 10 °C/min to the previous with TGA determined safe temperature. An empty sample pan was weighed and used as reference to the heat capacity of the pans.

The mDSC instrument settings for the heat capacity measurements were as follows: a modulation period of 100 s, a modulation amplitude of +/− 0.5 °K and an underlying heat rate of 1 °K/min. The heat capacity constant (KC_p) was calibrated using a sapphire disc weighing approximately 25 mg. Heat capacity measurements for the crystalline and amorphous compound were performed over a temperature range of 25 °C (absolute) to 20 °C above the melting point of NH. Analysis of the (m)DSC results was carried out with the Trios discovery evaluation software version v4.0.2.30774 (TA instruments).

2.7. Thermogravimetric analysis

Thermogravimetric analysis (TGA) was performed on a Q50 thermogravimetric analyzer (TA Instruments, New Castle, DE, USA). The weight change is measured as a function of time and/or temperature. A typical sample (+/− 10 mg) was placed on a platina sample holder and heated from room temperature to 1000 °C at heating rates of 2.5, 5, 10, 20 and 40 °K/min. Advantage software (TA Instruments) v5.5.22 was used for the analysis of the TGA data.

3. Theory and calculations

3.1. Thermodynamics of the amorphous state

The thermodynamic fragility F_T of amorphous NH was evaluated from the heat capacity change at the glass transition temperature (T_g) using Eq. 1 [12]: $F_T = \frac{C_p^{conf}}{\Delta C_p}$ where $C_p{}^{conf}$ is the heat capacity difference between the crystalline and the amorphous drug (J/mol/°K), the configurational heat capacity and ΔC_p is the change in heat capacity of the amorphous drug at T_g.

The Kauzmann temperature (T_k) was calculated using the different Eq. 2a: $T_{k1} \approx \frac{(T_g)^2}{T_m}$, Eq. 2b: $T_{k2} = T_g - 50$, and Eq. 2c: $\frac{1}{T_{k3}} = \frac{1}{T_m}\left(1 + \frac{\Delta H_m}{K}\right)$

The K-value (J/mol) in equation 2c was determined using the relationship expressed in Eq. 3: $K = C_p^{conf} * T$

Temperature-independency of K was verified by plotting $C_p{}^{conf}$*T versus T.

The dynamic fragility of amorphous NH was analysed by two different methods. The first method utilizes the Vogel-Tammann-Fulcher relation to calculate the strength parameter D_1 (−) through Eq. 4: $\Gamma = \Gamma_0 \exp\left(\frac{D_1 T_0}{T - T_0}\right)$ where Γ is the molecular relaxation time (s), Γ_0 is the vibrational lifetime of approximately 10^{-14} seconds (s) and T_0 is the constant Vogel temperature. Using this method assumes that T_k from Eq. (2)c and T_o have roughly the same value and also the value of Γ at T_g is approximately 100 s.

The strength parameter was subsequently used to calculate the fragility parameter m_1 (−) using Eq. 5 [13]: $m_1 = \frac{D_1 T_0}{T_g(\ln 10)\left(1 - \frac{T_0}{T_g}\right)^2}$

The second method uses the different values of T_g that are measured at various heating rates β (°K/min).

Through the linear relationship between the inverse values of the measured T_g's and the natural logarithm of the heating rate, the glass transition activation energy, ΔE_{Tg} (kJ/mol) can be calculated using Eq. 6 [13]: $-\frac{\Delta E_{Tg}}{R} = \frac{d \ln \beta}{d(1/T_g)}$ Where R is the universal gas constant (J/°K/mol). The fragility parameter, m_2, and the strength parameter, D_2, can then be determined by using Eq. 7: $m_2 = \frac{\Delta E_{Tg}}{\ln 10 * R * T_g}$, and Eq. 8: $D_2 = \frac{2.303\left(m^2_{min}\right)}{m_2 - m_{min}}$ Where m_{min} is the logarithm of the ratio of the mean relaxation time at T_g and the vibrational lifetime for which the value is 16 [13]. These fragility parameters allow the calculation of the Vogel temperature using Eq. 9: $T_0 = T_g\left(1 - \frac{m_{min}}{m_2}\right)$

T_0 was reintroduced in Eq. (4) to calculate relaxation times at different temperatures.

The enthalpic driving force H_c (kJ/mol) and the configurational entropy S_c (J/mol/°K), were calculated with Eq. 10: $H_c = \Delta H_m + \int_{T_m}^{T} C_p^{conf} dT$, and Eq. 11: $S_c = \Delta S_m + \int_{T_m}^{T} \frac{C_p^{conf}}{T} dT$ where: $\Delta S_m = \frac{\Delta H_m}{T_m}$, ΔH_m and ΔS_m are the enthalpy and entropy of melting as determined by DSC (J/mol and J/mol/°K), T is temperature (°K), T_m is melting temperature (°K) [14].

The overall force for crystallisation (Gibbs free energy) G_c (kJ/mol) was derived from Eq. 13: $G_c = H_c - (S_c * T)$

3.2. Thermal decomposition parameters

The results from the TGA analyses at different heating rates were evaluated with both the Ozawa-Flynn-Wall (OFW) and Friedman (F) isoconversional methods. These kinetic methods propose that the isothermal rate of conversion, dα/dt, is a linear function of the temperature, the rate constant, k(T), and a temperature-independent conversion function, f(α), Eq. 14: $\frac{d\alpha}{f(\alpha)} = \left(\frac{A}{\beta}\right) * e^{-E_a/RT} dT$ where β is the heating rate in °K/min, A, the pre-exponential factor and E_a the activation energy [11].

The OFW and the F methods can be utilized to calculate E_a. The methods are based on the assumption that for every value of α, f(α) is not dependent on the heating rate. It is then a requirement to measure α at different heating rates. Eq. (14) under these conditions can be rewritten as Eq. 15 for OFW: $\ln \beta = \ln \frac{AE_a}{R} - 5.331 - 1.052 \frac{E_a}{RT}$ and as Eq. 16 for F [15]: $\ln\left(\beta \frac{d\alpha}{dT}\right) = \ln A f(\alpha) - \frac{E_a}{RT}$

When plots are constructed of lnβ and ln(βdα/dt) against 1/T a linear relationship should be found. The slope of the linearity can then be used to calculate E_a and A. The estimation of the pre-exponential factor was carried out in the assumption that the kinetics of the decomposition process can be described by the phase-boundary model (R2), with kinetic exponent n=2 and a four degree 'rational approximation' [16].

The change of entropy, $H^{\neq}$ (kJ/mol), enthalpy, $S^{\neq}$ (J/mol/°K), and Gibbs free energy, $G^{\neq}$ (kJ/mol), for the formation of the activated complex were calculated using Eq. 17: $\Delta S^{\neq} = R \ln \frac{Ah}{e\chi k T_p}$, Eq. 18: $\Delta H^{\neq} = E - RT_p$, and Eq. 19: $\Delta G^{\neq} = \Delta H - T_p \Delta S$ where h = Planck's constant (J·s), e = Np (Euler's) number (−), χ = transition factor (−), k = Boltzmann constant ($J \cdot K^{-1}$), T_p = peak temperature of the DTG curve (°K).

4. Results and discussion

4.1. Nuclear magnetic resonance spectroscopy (NMR)

^1H- and ^{13}C NMR spectra were recorded of NH monohydrate, before and after spray drying. Supplementary Table S1 available at the online version at DOI: 10.1016/j.jpba.2017.10.001 presents the proposed assignments of the NMR-signals for both spectra. The NMR-spectra showed no significant change after spray drying, suggesting conservation of the NH molecular structure.

4.2. Fourier transform infrared spectroscopy (FTIR)

FTIR spectra were recorded of NH monohydrate, NH and spray-dried NH. The spectra are presented in Fig. 1a. The obtained results for all drug forms show similarity in the characteristic bands as listed in Supplementary Table S1 available at the online version at DOI: 10.1016/j.jpba.2017.10.001. The similarity in the spectra of NH monohydrate and NH is indicative of resembling molecular interaction between the drug molecules with and without the presence of water of crystallization.

The spectrum of the spray-dried NH displays a blue shift and an increase in transmittance for the bands corresponding to the C-F stretch (1085, 1118, 1228, 1261 and 1292 cm^{-1}), the C=O stretch (1585 cm^{-1}) and the C—N stretch (1540 cm^{-1}) relative to the NH spectrum. Additionally, the bands corresponding to N—H stretches (2964, 3055, 3209 cm^{-1}) demonstrate less intensity and broadening. These observations are suggestive of amorphization of NH. Furthermore, the spectra reveal that the mentioned bonds are of importance in maintaining the crystal structure of NH and in the recrystallization from the amorphous form.

4.3. Powder X-ray diffraction (XRD)

Fig. 1b presents the XRD spectra of NH monohydrate and spray dried material. The spectrum of NH monohydrate displays a sharp peak pattern that is characteristic of crystalline material and corresponds well to the spectrum of Form B [17]. This crystalline pattern is not observed in the spectrum of the spray dried material. This further indicates the successful amorphization of NH by spray drying.

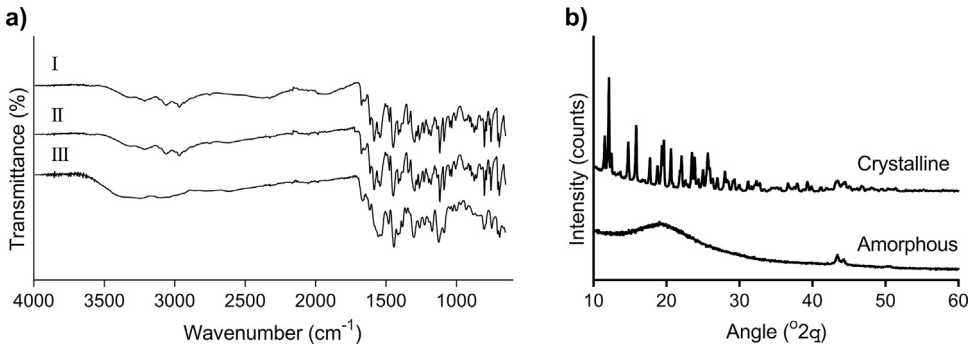

Fig. 1. Characterization results: a). FTIR spectra: I. crystalline NH monohydrate; II. crystalline NH; III. amorphous NH; b). XRD patterns of crystalline NH and amorphous NH;.

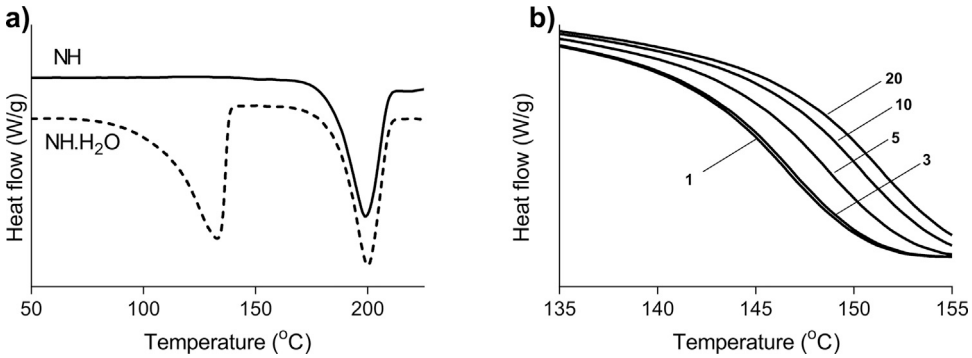

Fig. 2. DSC results: a). DSC curves of NH and NH monohydrate obtained at a heating rate of 10 °C/min; b). DSC curves of amorphous NH at heating rates of 1, 3, 5, 10 and 20 °C/min (indicated in figure), zoomed in on T_g.

4.4. (Modulated temperature) differential scanning calorimetry ((MT)DSC)

Fig. 2a represents the DSC curves of NH monohydrate and NH. Both curves show an endothermic peak that corresponds to the melting event (T_{peak} = 199.1 °C; T_{onset} = 194.2 °C). The melting enthalpy and entropy are listed in Table 1 and were found to be similar for both forms. The DSC curve of NH monohydrate exhibits a second endothermic peak (T_{peak} = 133.4 °C; T_{onset} = 97.81 °C) that corresponds to the loss of water of crystallization. These results show that the melting event is preceded by the transformation of the monohydrate to the anhydrate salt form, which is consistent with literature data [17].

The DSC curves of spray-dried NH recorded at different heating rates of 1, 3, 5, 10 and 20 °K/min are presented in Fig. 2b. The curves show an endothermic shift characteristic of glass transition ($T_{midmean}$ = 147.0 °C; $T_{onsetmean}$ = 145.2 °C). The measurements were repeated with in situ amorphisized (quench cooled) NH. The observed T_g was similar to that of spray-dried material ($T_{midmean}$ = 146.7 °C; $T_{onsetmean}$ = 145.0 °C). This indicates that spray-dried material is not likely to contain significant plasticizing amounts of ethanol or water. This was confirmed by Karl Fischer titrations and gas chromatography.

The heat capacities of NH and spray-dried NH were measured by mDSC from 25 °C to 220 °C. Fig. 3a shows the difference between these capacities, the configurational heat capacity (C_p^{conf}). The ΔC_p^{conf} during glass transition was found to be 161 J/mol/° K. This relatively large increase in ΔC_p^{conf} signifies fast relaxation during glass transition (i.e. fragile behaviour) of amorphous material/glass. This is in line with the generalized notion that pharmaceutical solids characterize as fragile glasses [18].

4.5. Thermodynamics of the amorphous state

Table 1 lists the calculated thermodynamic parameters of the amorphous state of NH.

The parameters F_T and m_1, D_1, m_2 and D_2 are all below or above the respective reference values for strong glass behaviour (F_T > 1.5; D > 30; m < 40). These results indicate that amorphous NH is likely to be a fragile system. This is in agreement with the observed ΔC_p^{conf}.

The T_k values display a range of approximately 40 °C, which is consistent with observations in literature [19]. The T_k values, as indicators for negligible molecular mobility, imply amorphous stability at typical storage temperatures (20–25 °C).

Γ was found to be near 100 s at T_g and found to increase exponentially as temperature decreases (Fig. 3b). This corresponds to literature data on fragile amorphous systems [13].

Fig. 3c–e presents H_c, S_c, and G_c in relation to reduced temperature. The observed trends and values of the parameters are thought to correspond to a reduced tendency to crystallize [20]. The results suggest amorphous NH to be a stable, fragile system. These are desirable characteristics from a pharmaceutical point of view.

4.6. Thermogravimetric analysis

Fig. 4a presents the TGA curve at heating rates of 2.5, 5, 10, 20 and 40° K/min and the DTG curve. The figure shows that the thermolytic degradation takes place in two distinct phases. Table 1 lists the thermal decomposition parameters of both phases at 10° K/min: the extrapolated onset temperature of degradation (T_{onset}); the temperature at which 0.5% mass loss occurs ($T_{0.5\%}$); the temperature at maximum weight loss rate (T_{max}); the extrapolated temperature at

Table 1
Summary of the thermal properties of crystalline and amorphous NH.

Parameter	Value	Parameter	Value	Parameter	Value	
T_m (°C)	199	Phase I		E_a (kJ/mol) Ozawa-Flynn-Wall	Phase I	Phase II
ΔH_m (kJ/mol)	32.5	T_{onset} (°C)	216	Friedman		
ΔS_m (J/mol/°K)	70.6	$T_{0.5\%}$ (°C)	193		103	205 197
					91.4	
		T_{max} (°C)	248			
T_g (°C)	147	T_{end} (°C)	294	A (s^{-1}) Ozawa-Flynn-Wall		
ΔC_p (J/mol/°K)	161	res (%)	93.6	Friedman	$5.6*10^6$	$4.7*10^{11}$
F_T (−)	1.31	Phase II			$1.6*10^6$	$3.3*10^{11}$
T_{k1} (°C)	108	T_{onset} (°C)	325	$H^{\neq}$ (kJ/mol)		
T_{k2} (°C)	97	T_{max} (°C)	434	Ozawa-Flynn-Wall Friedman	98.4	198
T_{k3} (°C)	65	T_{end} (°C)	546		87.1	190
T_m/T_g (−)	1.10	res (%)	20.4	$S^{\neq}$ (J/mol/°K)		
D_1 (−)	9.07			Ozawa-Flynn-Wall Friedman	−129	−36.9
m_1 (−)	80.9				−139	−40.5
ΔE_{Tg} (kJ/mol)	558			$G^{\neq}$ (kJ/mol)		
D_2 (−)	11.0			Ozawa-Flynn-Wall Friedman	165	226
m_2 (−)	69.4				159	221
T_0 (°C)	50.2					
Γ at T_g (s)	89.2					
H_c at T_g (kJ/mol)	24.0					
S_c at T_g (J/mol/°K)	51.2					
G_c at T_g (kJ/mol)	2.82					

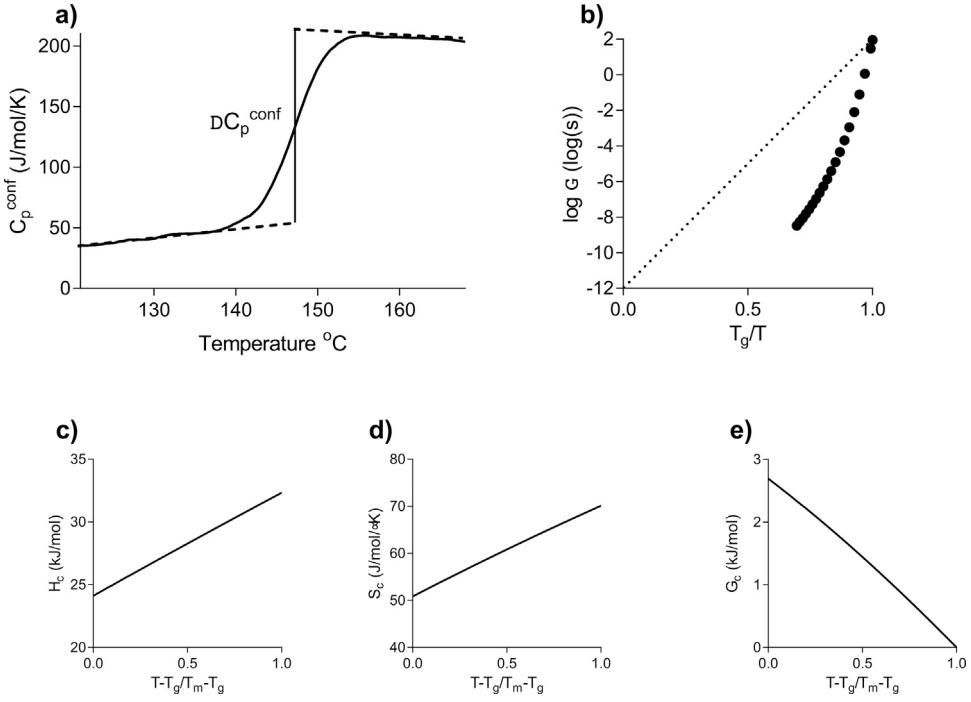

Fig. 3. mDSC results: a). C_p^{conf} as a function of the temperature of amorphous NH. Indicated is the determination of ΔC_p; b). Calculated values for Γ up to T_g for amorphous NH. The dotted line represents the ideal strong behaviour, deviations from linearity signify fragility; c–e). Configurational thermodynamic properties of amorphous NH as a function of the reduced temperature, where 0 equals T_g and 1 equals T_m: c. H_c; d. S_c; e. G_c.

which the degradation process end (T_{end}); the amount of residue at T_{end} (res%).

The thermograms show a trend of movement towards higher temperatures with increasing heating rate. This can be attributed to a delay in thermal degradation and an increase in thermal lag.

At a heating rate of 10° K/min, NH is stable up to 193 °C ($T_{0.5\%}$). This is below the T_m of 199 °C, which indicates that melting is accompanied by partial drug degradation. In the first phase a weight loss of 6.4% (±0.5%) occurs. This can be attributed stoichiometrically to the loss of hydrochloride (6.4% (w/w)). The second phase involves a weight loss of 68.9% (w/w). This is likely to resemble the degradation of a large part of the aromatic backbone of the drug structure.

4.7. Thermal decomposition parameters

The calculated thermal degradation parameters are listed in Table 1.

Fig. S2 shows the isoconversional plots of the two degradation phases based on the OFW model and the isoconversional plots

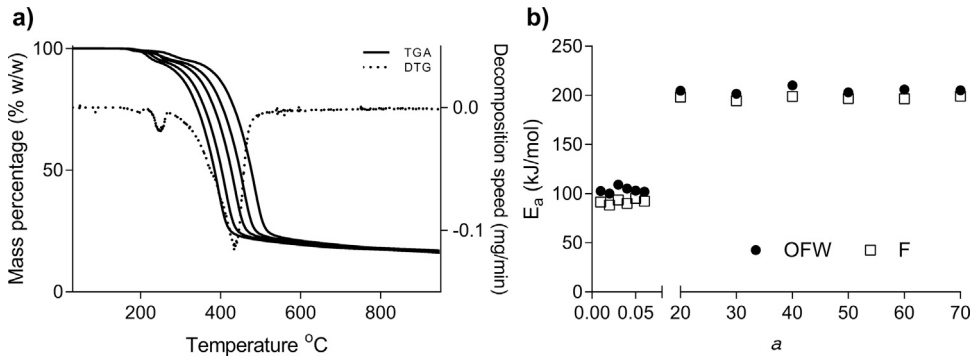

Fig. 4. TGA results: a). TGA (solid) and DTG (dotted; 10 °C/min) curves of crystalline NH obtained at heating rates of 2.5, 5, 10, 20 and 40 °C/min (indicated in figure); b). The mean values of E_a plotted to α calculated by OFW and F.

according to the F model are presented in Supplementary Fig. S2 available at the online version at DOI: 10.1016/j.jpba.2017.10.001.

The E_a values from both methods are shown as a function of α in Fig. 4b. The resulting E_a values vary between the two methods. This may be due to the different temperature integral approximations of the methods. The obtained E_a values from methods showed consistency within the phases of degradation. This suggests that the non-isothermal degradation phases are single-step processes.

The values of $\Delta S^{\neq}$, $\Delta H^{\neq}$ and $\Delta G^{\neq}$ are dependent on the choice of the reaction model, which is in turn dependent on the particle shape and diffusion characteristics. This is beyond the scope of this analysis and should be the subject of future studies.

Thermal degradation can additionally be studied by using isothermal methods. In this case, such an approach is not feasible because of the two degradation phases that may interfere during isothermal heating.

4.8. Physical stability

To experimentally assess the physical stability of amorphous NH, amorphous material was analysed isothermically by DSC at temperatures between T_g and T_m. Drug material was kept at 150, 155, 160, 165, 170, 175 and 180 °C for 5 h. During these periods, no exothermic event was observed that could indicate crystallization. Additionally, T_gs were still present during reanalysis. These observations are in agreement with the thermodynamic parameters that indicate amorphous stability.

To study any physical changes in the bulk amorphous material under storage conditions, the material was kept in the dark at 20–25 °C and a relative humidity of 60%. Analyses were performed with Karl Fisher titration, XRD and DSC at regular time intervals. Supplementary Table S2 available at the online version at DOI: 10.1016/j.jpba.2017.10.001 presents the results up to 6 months of storage. The amorphous material attracts water up to 0.54% over time but does not seem to destabilize because of it, at least up to 6 months.

5. Conclusions

This study presents the thermal stability analysis of crystalline NH monohydrate, NH and spray-dried amorphous NH. The resulting thermal characteristics of NH can be used to evaluate the pharmaceutical quality and to further understand the response of the drug to thermal stress during processing and storage. The spray drying amorphization procedure was monitored by NMR, FTIR and XRD techniques. The method was shown to produce amorphous NH without drug degradation.

The amorphous phase of NH has been characterized with respect to thermodynamic and molecular mobility both above and below T_g. The thermodynamic properties indicate a fragile amorphous phase and low crystallization tendency.

The thermal degradation of NH takes places in two phases. The initial degradation temperature was found to 193 °C, below the T_m of 199 °C. The obtained results from TGA were evaluated using non-isothermal, model-free isoconversional methods. The derived E_a values are consistent with single-step degradation processes for both phases.

The examination of the physical stability of amorphous NH during storage and at elevated temperatures showed stability at 180 °C for at least 5 h and at 20–25 °C/60% RH for at least 6 months.

The results from this study demonstrate that crystalline and amorphous NH may be regarded as relatively stable drug phases. In conclusion, NH is a suitable candidate for new formulation studies where thermal production methods are utilized such as hot-melt extrusion and spray drying.

Future studies should focus on the stability of newly developed formulations with amorphous NH.

References

[1] US Food and Drug administration (FDA), Prescribing Information Tasigna(R), 2010.
[2] F.X. Mahon, S. Hayette, V. Lagarde, F. Belloc, B. Turcq, F. Nicolini, C. Belanger, P.W. Manley, C. Leroy, G. Etienne, S. Roche, J.-M. Pasquet, Evidence that Resistance to Nilotinib May Be Due to BCR-ABL Pgp, or Src Kinase Overexpression, Cancer Res. 68 (2008) 9809–9816.
[3] B.C. Hancock, G. Zografi, Characteristics and significance of the amorphous state in pharmaceutical systems, J. Pharm. Sci. 86 (1997) 1–12.
[4] G. Jesson, M. Brisander, P. Andersson, M. Demirbüker, H. Derand, H. Lennernäs, M. Malmsten, Carbon dioxide-mediated generation of hybrid nanoparticles for improved bioavailability of protein kinase inhibitors, Pharm. Res. 31 (2014) 694–705.
[5] P. Andersson, M. Von Euler, M. Beckert, Comparable pharmacokineties of 85 mg RightSize nilotinib (XS003) and 150 mg Tasigna in healthy volunteers using a hybrid narioparticle-based formulation platform for protein kinase inhibitors, 2014 ASCO Annu. Meet. (2014).
[6] S. Gupta, R. Kesarla, A. Omri, Formulation strategies to improve the bioavailability of poorly absorbed drugs with special emphasis on self-emulsifying systems, ISRN Pharm. 2013 (2013) 848043.
[7] J. Li, D. Patel, G. Wang, Use of spray-dried dispersions in early pharmaceutical development: theoretical and practical challenges, AAPS J. 19 (2017) 321–333, http://dx.doi.org/10.1208/s12248-016-0017-9.
[8] D. Giron, Contribution of thermal methods and related techniques to the rational development of pharmaceuticals—part 1, Pharm. Sci. Technol. Today 1 (1998) 191–199.
[9] S. Bajaj, D. Singla, N. Sakhuja, Stability testing of pharmaceutical products, J. Appl. Pharm. Sci. 2 (2012) 129–138.
[10] L.X. Yu, G. Amidon, M.A. Khan, S.W. Hoag, J. Polli, G.K. Raju, J. Woodcock, Understanding pharmaceutical quality by design, AAPS J. 16 (2014) 771–783.
[11] S. Vyazovkin, A.K. Burnham, J.M. Criado, L.A. Pérez-Maqueda, C. Popescu, N. Sbirrazzuoli, ICTAC Kinetics Committee recommendations for performing kinetic computations on thermal analysis data, Thermochim. Acta. 520 (2011) 1–19.
[12] D. Huang, G.B. McKenna, New insights into the fragility dilemma in liquids, J. Chem. Phys. 114 (2001) 5621.
[13] K.J. Crowley, G. Zografi, The use of thermal methods for predicting glass-former fragility, Thermochim. Acta. 380 (2001) 79–93.

[14] K.A. Graeser, J.E. Patterson, J.A. Zeitler, K.C. Gordon, T. Rades, Correlating thermodynamic and kinetic parameters with amorphous stability, Eur. J. Pharm. Sci. 37 (2009) 492–498.
[15] H.L. Friedman, Kinetics of thermal degradation of char-forming plastics from thermogravimetry. Application to a phenolic plastic, J. Polym. Sci. Part C Polym. Symp. 6 (2007) 183–195.
[16] J.H. Flynn, The temperature integral — its use and abuse, Thermochim. Acta. 300 (1997) 83–92, http://dx.doi.org/10.1016/S0040-6031(97)00046-4.
[17] P.W. Manley, W.-C. Shieh, P.A. Sutton, P.H. Karpinski, Crystalline forms of 4-methyl-n-[3-(4-methyl-imidazol-1-yl)-5-trifluoromethyl-phenyl]-3-(4-pyridin-3-yl-pyrimidin-2-ylamino)-benzamide, WO2007015870A2, 2005.
[18] C.A. Angell, Entropy and fragility in supercooling liquids, J. Res. Natl. Inst. Stand. Technol. 102 (1997) 171.
[19] A. Kaushal, A. Bansal, Thermodynamic behavior of glassy state of structurally related compounds, Eur. J. Pharm. Biopharm. 69 (2008) 1067–1076.
[20] D. Zhou, G.G.Z. Zhang, D. Law, D.J.W. Grant, E.A. Schmitt, Physical stability of amorphous pharmaceuticals: importance of configurational thermodynamic quantities and molecular mobility, J. Pharm. Sci. 91 (2002) 1863–1872.